Neuron, volume *60*

Supplemental Data

Interaction between Reelin and Notch Signaling Regulates Neuronal Migration in the Cerebral Cortex

Kazue Hashimoto-Torii, Masaaki Torii, Matthew R. Sarkisian, Christopher M. Bartley, Jie Shen, Freddy Radtke, Thomas Gridley, Nenad Šestan, and Pasko Rakic

Figure S1

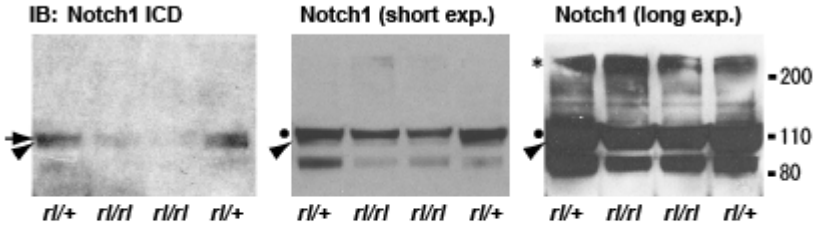

Figure S1.
Notch ICD was specifically reduced in *Reeler*.
Left photo shows a whole gel photo of Figure 1I. Arrow and arrowhead in immunoblot with anti-Notch1 ICD (Val 1744) indicate p120 phosphorylated and p110 non-phosphorylated Notch1 ICD respectively (Redmond et al., 2000 [see ref. list in the main text]). Subsequent immunoblot with anti-Notch1 (intracellular domain of Notch1 for antigen) detect p300 full-length Notch1 (asterisk in long exposure blot), p120 (filled circles), and p110 (arrowheads) Notch1 ICD. Similar to the blot using anti-Notch1 ICD, p110 Notch1 ICD band was decreased in the Notch1 blot. According to a previous report (Redmond et al., 2000, Tokunaga et al., 2004, J. Neurochem., *90*, 142-154), the p120 band in the Notch1 blot includes not only phosphorylated Notch1 ICD but also membrane-tethered Notch1 prior to ligand-stimulated cleavage. Considering the significant decrease in phospho-Notch1 ICD as seen in Notch1 ICD blot, the slight decrease in p120 band of *rl/rl* indicates that the amount of membrane-tethered Notch1 precursor before cleavage may be slightly affected in *rl/rl*.

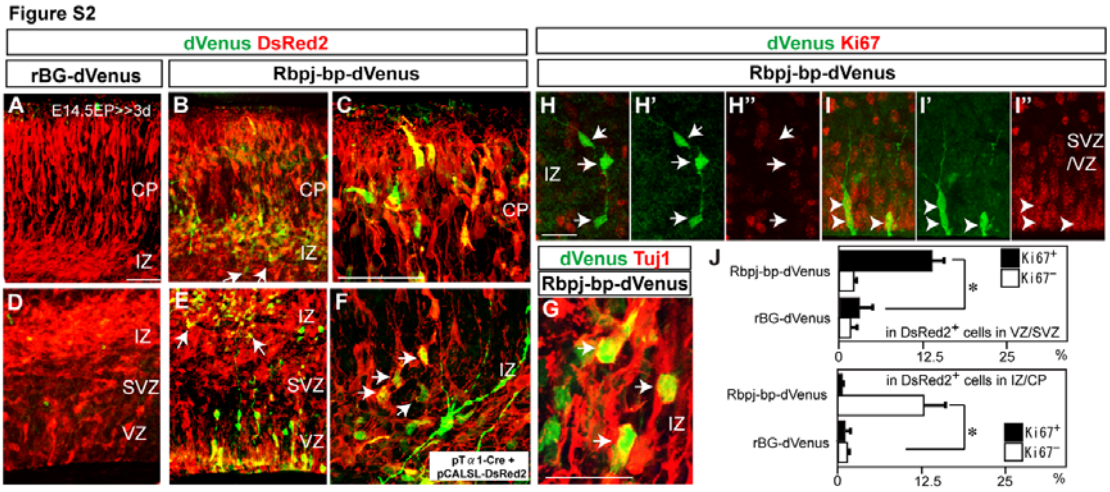

Figure S2.

Activation of Rbpj transcriptional function during neuronal migration.

(A-F) Immunostaining for dVenus (green) and DsRed2 (red) around the IZ/CP (A-C, F) or VZ/SVZ (D, E) 3 days post-electroporation at E14.5 in wild-type cortex with indicated reporter plasmids, together with pCAG-DsRed2 (A-E) or pTα1-Cre and pCALSL-DsRed2 for labeling of post-mitotic neurons (F). (C) is higher magnification view around upper CP in (B). Rbpj-bp-dVenus encodes dVenus (a fusion of Venus [an EGFP variant] and a PEST domain which accelerates its degradation) under the control of the Rbpj-bp promoter (which harbors Rbpj binding sites with minimal promoter). (A, D) The reporter expression was barely detected by the electroporation of rBG (minimal promoter only)-dVenus, a control reporter construct. Arrows in B, E indicate reporter expression in the IZ. (F) Colocalization of dVenus and Tα1 promoter-driven DsRed2 (arrows) indicates that the reporter is activated in migrating neurons. (G) Immunostaining of dVenus (green) with the neuronal marker Tuj1 (red) in the IZ in wild-type, showing reporter expression in migrating post-mitotic neurons (arrows). (H-I'') Immunostaining of dVenus (green) with the proliferation marker, Ki67 (red) in the IZ (H-H'') or VZ/SVZ (I-I'') in wild-type. Arrows and arrowheads indicate reporter expression in post-mitotic and progenitor cells respectively. (J) Percentages of $Ki67^+/dVenus^+$ (black bars) and $Ki67^-/dVenus^+$ (white bars) cells in $DsRed2^+$ cells electroporated with indicated plasmids and pCAG-DsRed2 in the VZ/SVZ (upper panel) or IZ/CP (lower panel). The majority of $dVenus^+$ cells in the VZ/SVZ colocalized with Ki67 (I-I'', J) and Nestin (data not shown). Most $dVenus^+$ cells in the IZ/CP were Ki67 negative (H-H'', J), Tuj1-positive post-mitotic neurons (G). The data represent the mean ± SEM of 6 brains from independent experiments. $p<0.01$, Student's t-test. We also confirmed Notch reporter activity in migrating neurons in the reporter transgenic mice recently developed (data not shown)(Duncan et al., 2005, Nature Immunology, 6, 314-22). Bars (μm) = 50 (A-F), 20 (G-I'').

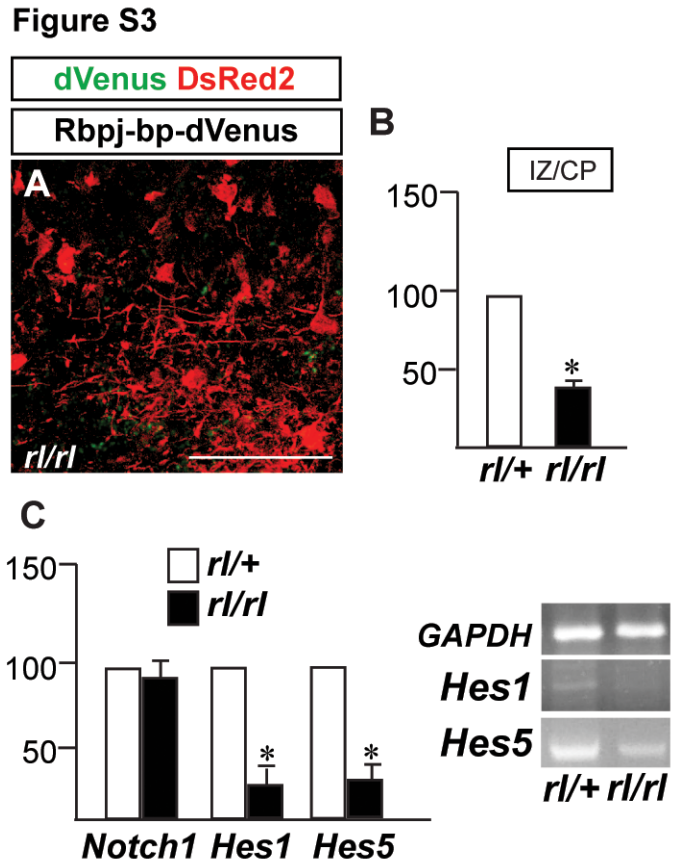

Figure S3.
Reduction of Rbpj transcriptional function in *Reeler*.
(A) Immunostaining for dVenus (green) and DsRed2 (red) 3 days post-electroporation at E14.5 in *Reeler* (*rl/rl*) cortex with Rbpj-bp-dVenus and pCAG-DsRed2 around CP. (B) The percentage of dVenus expressing cells in DsRed2^{+} (electroporated) cells in IZ and CP was quantified, and normalized to that of heterozygote littermates set as 100. The data represent the mean ± SEM of 4 brains from independent experiments. *$p<0.001$ by paired t-test. Bar (μm) = 50. (C) Quantitative real-time RT-PCR analysis of *Notch1*, *Hes1* and *Hes5* mRNA expression from E18.5 *rl/+* and *rl/rl* cerebral cortex. *$p<0.01$ by paired t-test. The RT-PCR bands for *Hes1*, and *Hes5* were normalized to *GAPDH* levels in indicated mutants. The cycles of reaction are as follows: *GAPDH:* 16, *Hes1:* 24, *Hes5:* 24.

Figure S4

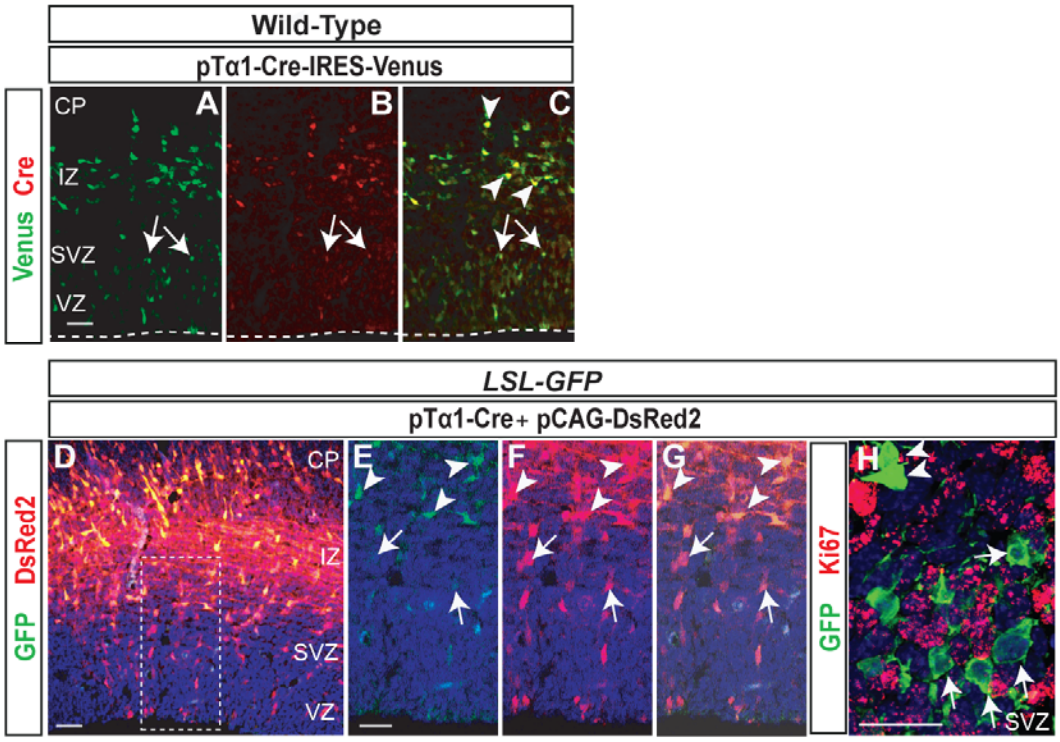

Figure S4.
Genomic recombination in newly-generated postmitotic neurons.
(A-C) Venus (green) and Cre recombinase (red) were detected by immunohistochemistry in coronal sections 2 days after electroporation with pTα1-Cre-IRES-Venus. Over 50% of Venus$^+$ cells express Cre recombinase strongly in the IZ (arrowheads). Very weak Cre expression is detected in the Venus$^+$ cells within the VZ (arrows), presumably the site where expression begins in immature neurons. (D-G) GFP (green) and DsRed2 (red) expression in the cortex of *LSL-GFP* mice 3days after electroporation of pTα1-Cre and pCAG-DsRed2. In *LSL-GFP* transgenic mice, GFP expression is induced by Cre-mediated recombination, while DsRed2 is ubiquitously expressed under CAG promoter in the electroporated cells. (E-G) Higher magnification views of the boxed area in (D). A few DsRed2$^+$ electroporated cells showed weak GFP expression in the SVZ (arrows in E-G), while strong GFP expression was observed in the IZ (arrowheads E-G). GFP expression was barely detectable in the VZ. (H) An adjacent section of (D) was immunostained with the anti-GFP (green) and anti-Ki67 (red). Neither the GFP$^+$ cells within (arrows) nor above (arrowheads) the SVZ colocalize with Ki67 (below 5%). Bars (μm) = 50 (A-D) and 25 (E-H). Dashed lines in (A-C) indicate the ventricular lining.

Figure S5

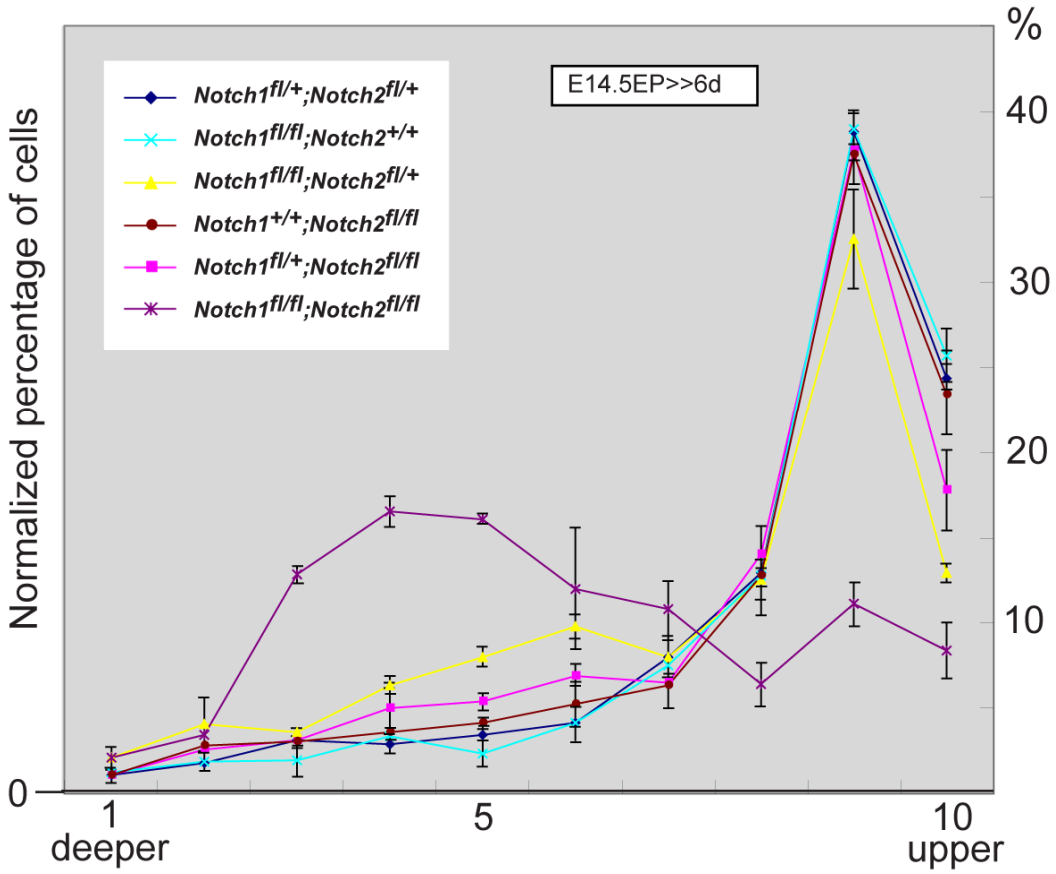

Figure S5.
Dose-dependent effects of the loss of Notch signaling on neuronal migration.
Quantification of Venus^{+} cell positioning in neocortex 6 days post-electroporation with pTα1-Cre-IRES-Venus in a series of *Notch1;Notch2 floxed* mice. *Notch1$^{fl/fl}$;Notch2$^{fl/fl}$* (purple) and *Notch1$^{fl/fl}$;Notch2$^{fl/+}$* (yellow) have significantly different distribution compared with *Notch1$^{fl/+}$;Notch2$^{fl/+}$* (dark blue) (*p<0.0001* by K-S test; Repeated measures ANOVA, F[9,36]=53.35, *p<0.0001* and F[9,36]=11.61, *p<0.0001*, respectively), while *Notch1$^{fl/fl}$;Notch2$^{+/+}$* (light blue) and *Notch1$^{+/+}$;Notch2$^{fl/fl}$*(brown) did not (*p>0.05* by K-S test; Repeated measures ANOVA, F[9,36]=0.41, *p>0.05* and F[9,36]=0.39, *p>0.05* respectively). A significant difference is detected between *Notch1^{fll+};Notch2$^{fl/fl}$* (pink) and *Notch1$^{fl/+}$;Notch2$^{fl/+}$* in their mean values (F[9,36]=3.11, *p<0.01* by Repeated measures ANOVA) but not in their distribution patterns (*p>0.05* by K-S test). The data represent the mean ± SEM of 3 brains each from independent experiments.

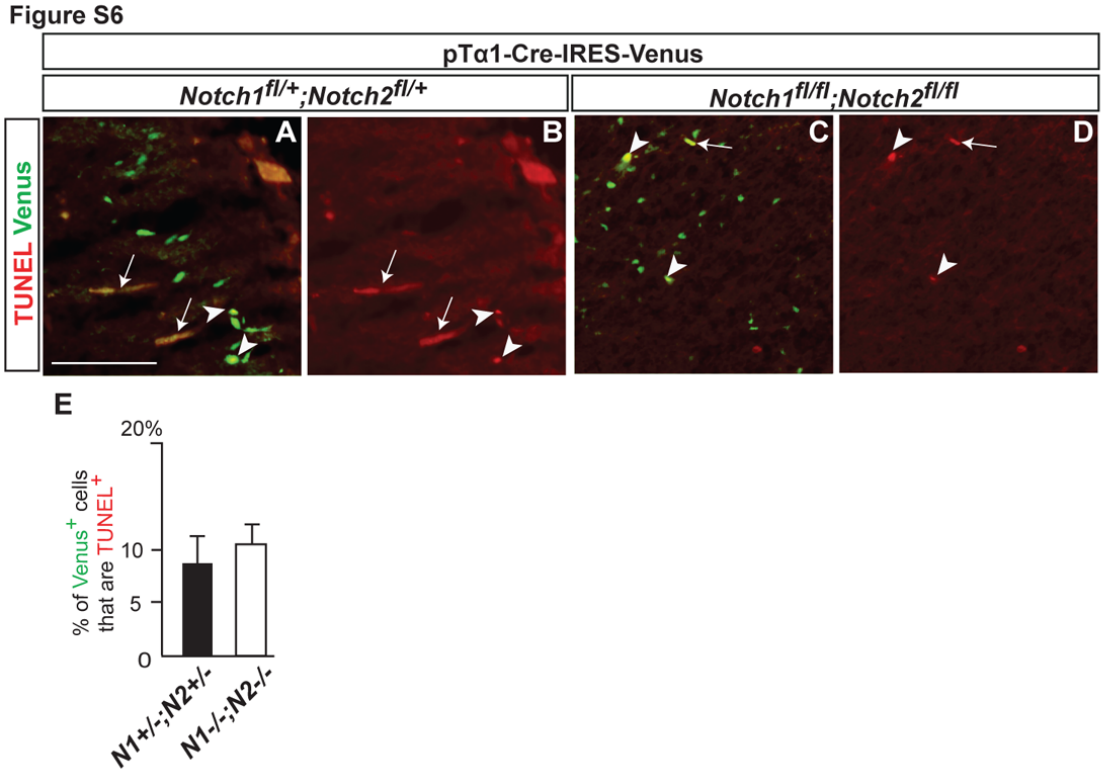

Figure S6.
Loss of Notch signaling does not affect the level of apoptosis.
(A-D) TUNEL analysis (red, A-D) combined with Venus (green, A, C) immunostaining was performed 4 days post-electroporation in indicated mutant mice with pTα1-Cre-IRES-Venus. Arrows indicate non-specific staining in the blood vessels. (E) The average percentage of $TUNEL^+$ /$Venus^+$ cells (as indicated by arrowheads in A-D) in $Venus^+$ cells was determined from 4 independent brains ($p>0.1$, Student's t-test). 6539 (homozygotes) and 7221 cells (heterozygotes) were counted from 4 brains each. Bar = 100 μm. Consistent with a previous study, Notch signaling seems to be not involved in the regulation of neuronal cell death, although it is critical in the precursor cells (Yang et al. 2004. Dev. Biol. *269:* 81-94; Mason et al. 2006. Dev. Neurosci. *28*: 49-57).

Figure S7

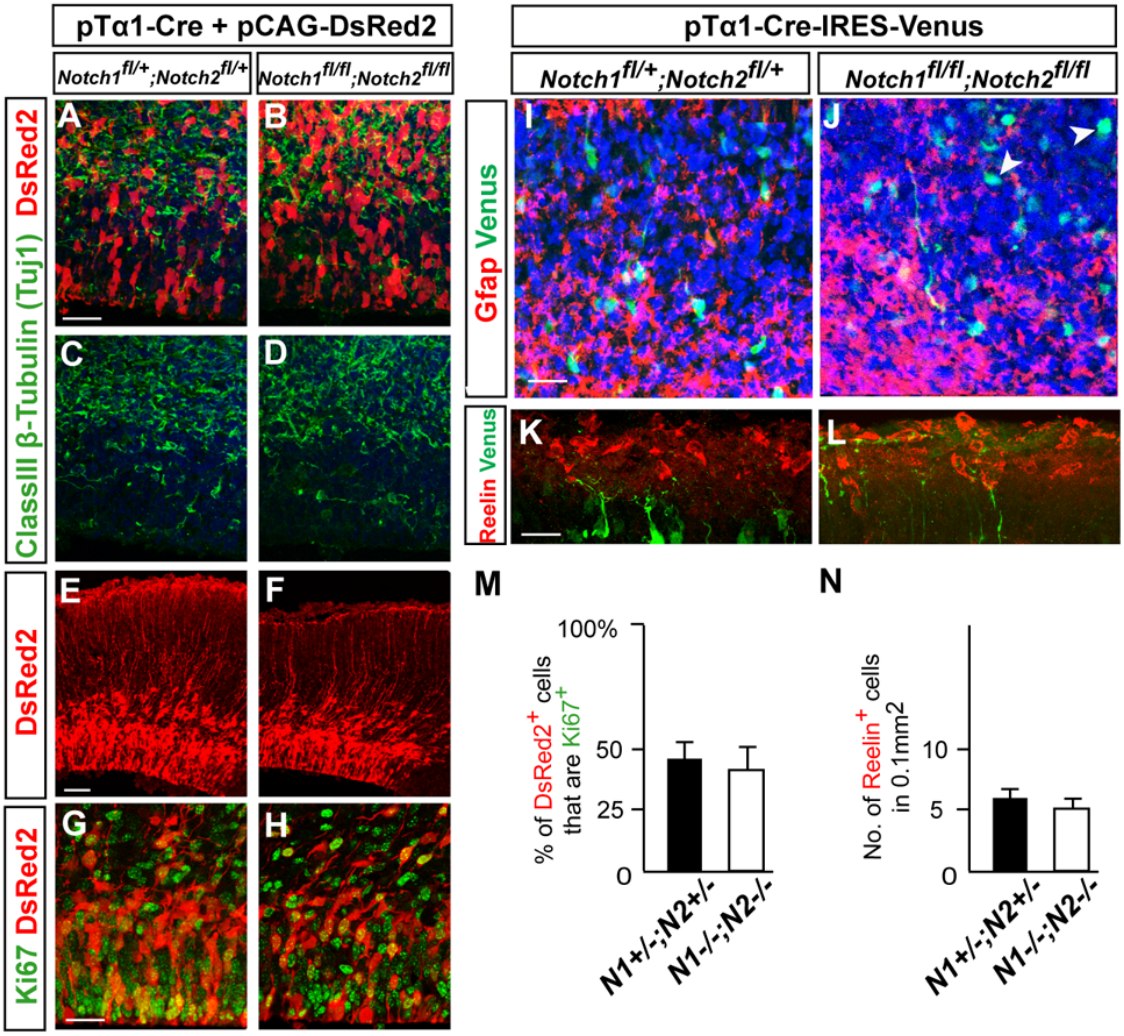

Figure S7.

Loss of Notch signaling does not affect the expression pattern of neuronal, glial or proliferation markers.

(A-L) Coronal cortical sections of the indicated floxed mice immunostained for the neuronal, glial or proliferation markers with the Venus or DsRed2; (A-D) class III β-tubulin (Tuj1, an early neuronal marker), (E, F) DsRed2 to show the morphology of radial glia, (G, H) Ki67 (proliferation marker), (I, J) Gfap (astroglial marker), and (K, L) Reelin. Staining was performed 2 days (A-D), 1 day (E-H), 3 days (I, J) 4 days (K, L) after electroporation of the indicated floxed mice with pTα1-Cre and pCAG-DsRed2 (a-h) or pTα1-Cre-IRES-Venus (I-L). Alteration of Tuj1 expression pattern was not observed in the electroporated region of double-targeted mice (A-D, n=6). No change of Gfap expression was observed in the electroporated cells in *Notch1;Notch2* double targeted mice (I, J, arrowheads, n= 4) The morphology of radial glia expanded in the CP appeared normal in homozygote as in heterozygotes, maintaining long processes that were attached to the basal membrane of the pia (E, F, n=4). (M) The ratio of $Ki67^+/DsRed2^+$ cells in double homozygotes was comparable to heterozygotes (G, H,

p>0.01, Student's t-test). 9235 (homozygotes) and 8520 cells (heterozygotes) were counted from 4 brains each. (N) The number of Reelin$^+$ cells in double homozygotes was comparable to heterozygotes (K, L, *p=n.s.* by Student's t-test, n=5). Bars (μm) = 100 (E, F), 20 (A-D, G-L).

Figure S8

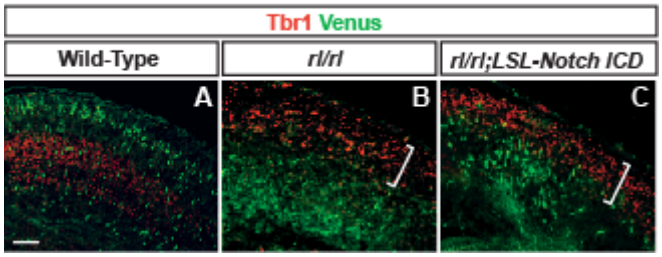

Figure S8.
Replenishing Notch ICD mitigates slower migration in *Reeler*.
(A-C) Immunohistochemical detection of Venus$^+$ (green) neurons with Tbr1 (red) 3.5 days post-electroporation in *rl/rl;LSL-Notch ICD* mice with pTα1-Cre-IRES-Venus. Brackets in (B, C) indicate the "inverted" Tbr1$^+$ early-born neuronal layer in *rl/rl* and *rl/rl;LSL-Notch ICD*. More neurons have reached and crossed the border of the Tbr1$^+$ layer in *rl/rl;LSL-Notch ICD* (C) than in *rl/rl* (B). n=3 each. Bars (μm) =100.

Figure S9

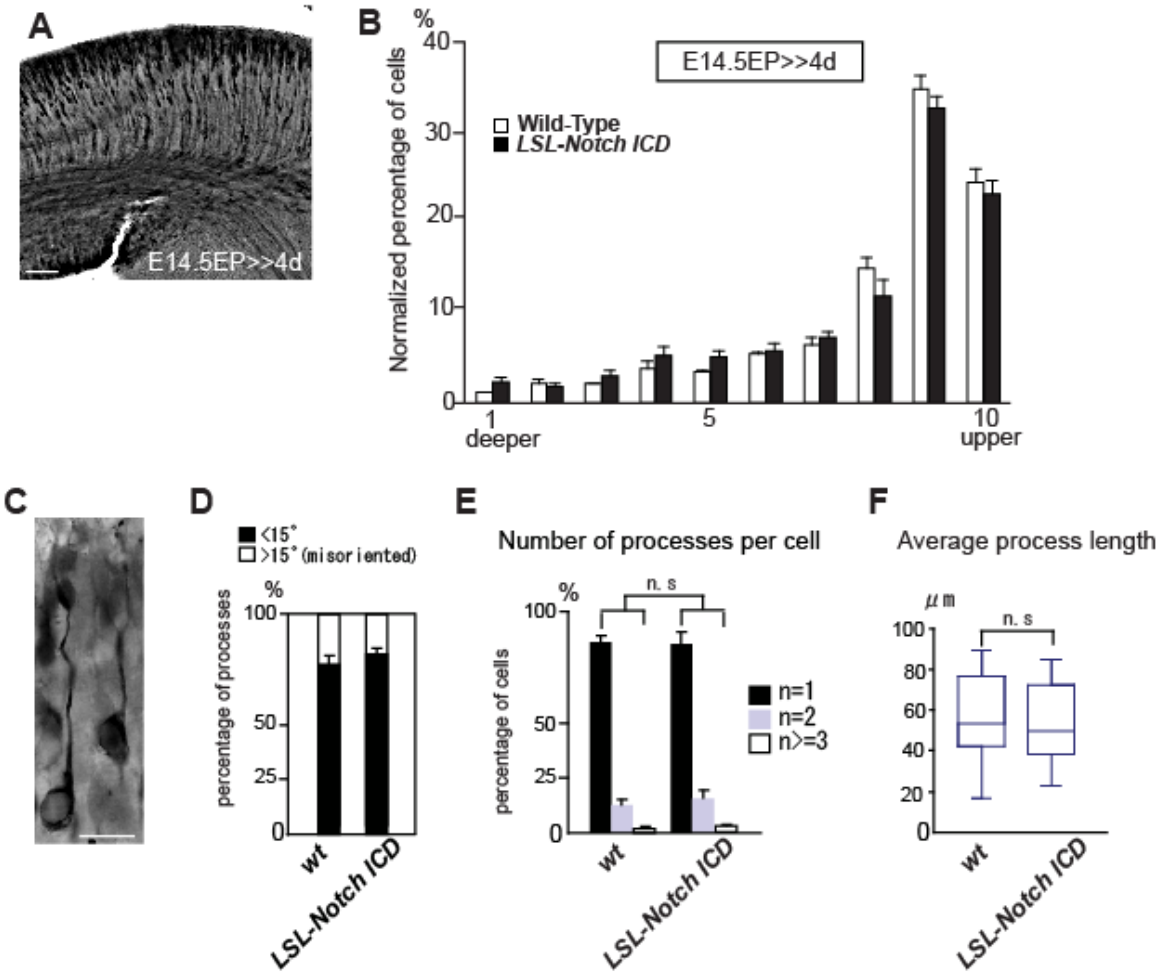

Figure S9.
Notch ICD overexpression does not affect positioning and morphology of migrating neurons.

(A, C) Immunohistochemical detection of Venus^{+} neurons 4 (A) and 3 (C) days post-electroporation in *LSL-Notch ICD* mice with pTα1-Cre-IRES-Venus. (B) Quantification of the positioning of neurons 4 days after electroporation in wild-type or *LSL-Notch ICD* mice with pTα1-Cre-IRES-Venus. The data represent the mean ± SEM of 4 brains from independent experiments. No significant differences between bins in two genotypes were observed (K-S test, $p>0.05$; Repeated Measures ANOVA $F(9,54)=1.31$, $p>0.05$). (D) The direction of primary processes was not misoriented ($p=n.s.$, compared with wild-type by Student's t-test). (E) Percentage of cells with indicated number of primary processes/cell. Thirty cells were counted from 4 independent experiments (total n=120). $p=n.s.$ for each corresponding column, according to Student's t-test. (F) Box plots of the primary process length per cell (total process length/number of the primary processes) (n=30 from 3 independent experimental sets). $p>0.05$, according to Mann-Whitney's U test. Quantification of the wild-type in (D-F) is duplicated from Figure 4 for comparison. Bars (μm) = 100 (A) and 10 (C).

Figure S10

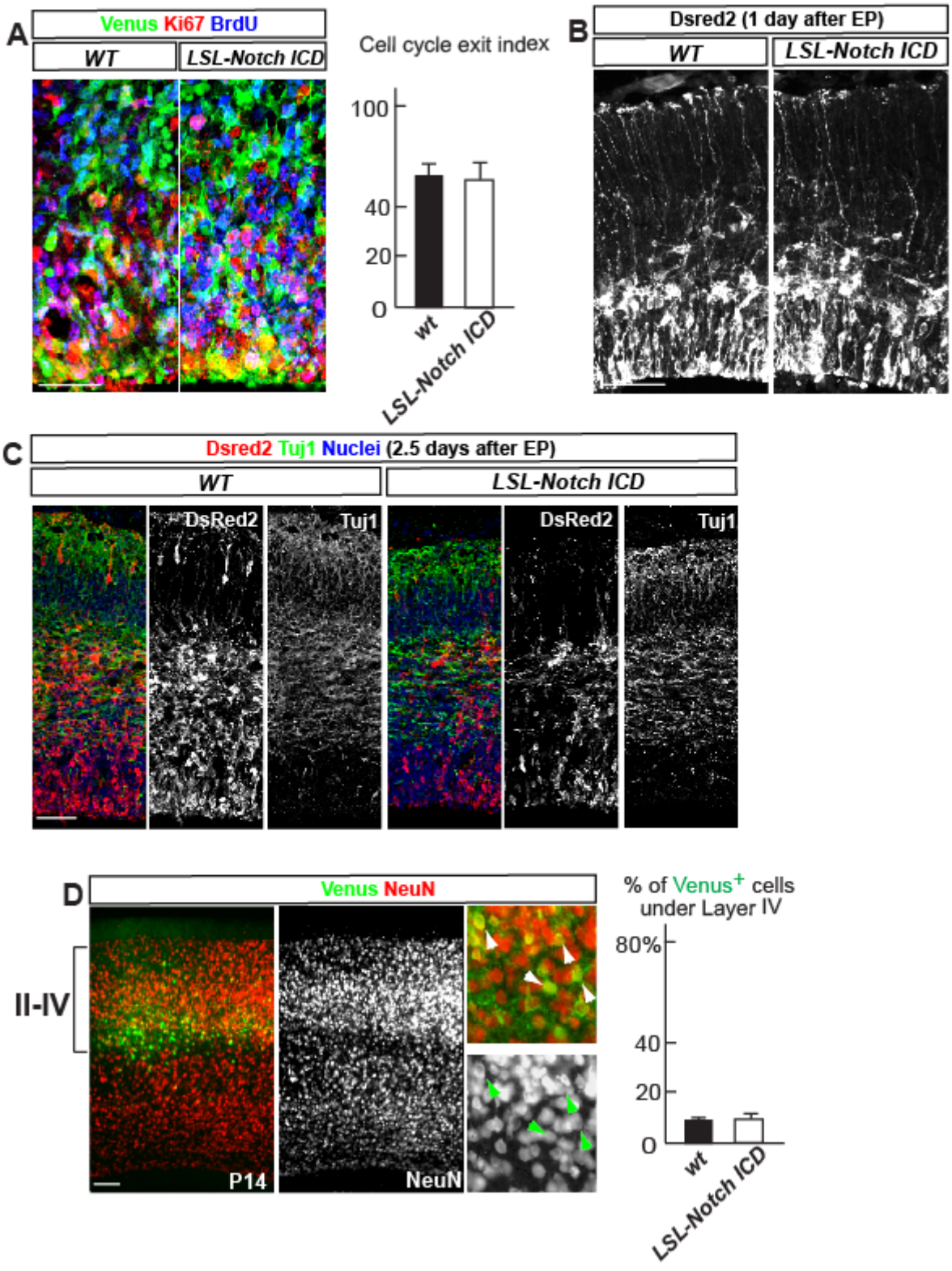
A
Venus Ki67 BrdU
WT
LSL-Notch ICD
Cell cycle exit index
100
40
20
0
wt
LSL-Notch ICD
B
Dsred2 (1 day after EP)
WT
LSL-Notch ICD
C
Dsred2 Tuj1 Nuclei (2.5 days after EP)
WT
LSL-Notch ICD
DsRed2
Tuj1
DsRed2
Tuj1
D
Venus NeuN
II-IV
P14
NeuN
% of Venus+ cells under Layer IV
80%
40
20
0
wt
LSL-Notch ICD

Figure S10.

Tα1 promoter driven Notch ICD overexpression does not affect neurogenesis and the final positioning of neurons.

(A) Left: Venus (green) immunostaining with Ki67 (red) and BrdU (blue) staining in indicated mice electroporated with pTα1-Cre-IRES-Venus at E14.5. BrdU was injected at E15.5 and brains were fixed at E16.5. Right: Cell cycle exit index (the percentage of $Ki67^-$ cells in $BrdU^+/Venus^+$ cells) indicates no difference between wild-type and *LSL-Notch ICD* mice. *p*=n.s. by Student's t-test. (B-C) Immunostaining for DsRed2 and Tuj1 1 day (B) and 2.5 days (C) after electroporation with pTα1-Cre and pCAG-DsRed2 in the indicated mice. The number and morphology of radial glia (B), and neurogenesis (C) were normal after neuron-specific Notch overexression. (D) Left: Venus (green) and NeuN (red or white) staining in P14 *LSL-Notch ICD* mouse electroporated with pTα1-Cre-IRES-Venus at E14.5. Right: Quantification shows no difference in the positioning of Notch ICD overexpressing neurons from the wild-type neurons (*p*=n.s., Student's t-test). Notch ICD overexpressing neurons were $NeuN^+$ (a neuronal marker, insets) but negative for GFAP (a marker for astrocyte) and RIP (a marker for oligodendrocyte)(data not shown). Bars (μm) = 50 (B and C), 25 (A) and 10 (C), 100 (D).

Figure S11

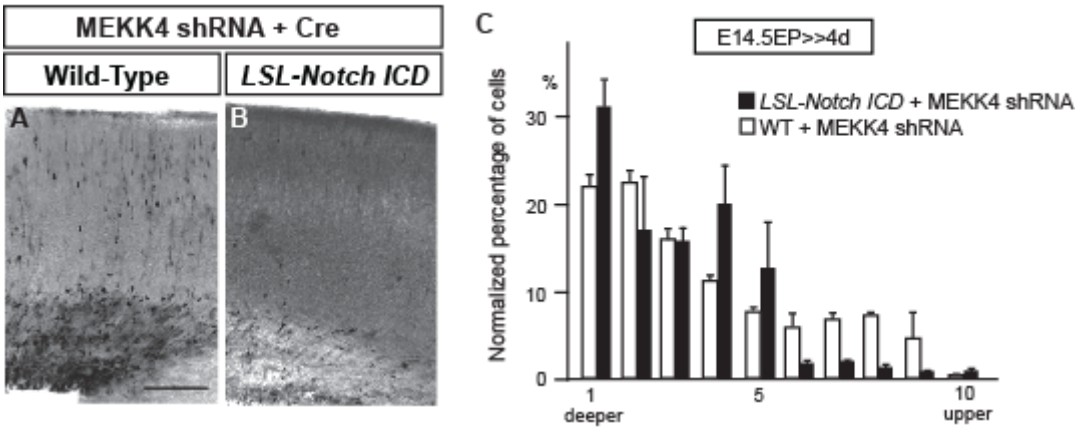

Figure S11.
Overexpression of Notch ICD did not mitigate migration defects caused by a Reelin-independent signaling pathway.
(A, B) Immunohistochemistry for Venus four days post-electroporation with MEKK4 shRNA plasmid and pTα1-Cre-IRES-Venus simultaneously in wild-type (A) or *LSL-Notch ICD* (B) cortex. Introduction of MEKK4 shRNA dramatically impaired neuronal migration to the cortical plate despite overexpression of Notch ICD. Severe reduction of cell density within the IZ, however, may imply a synergistic apoptotic effect. Bar = 100 μm. (C) Quantification of the distribution of neurons along the radial axis. The indicated average mean ± SEM is from 4 independent experiments. Overexpression of Notch ICD did not mitigate the dispositioning of the MEKK4 shRNA-electroporated neurons in deeper layers (Repeated Measures ANOVA, $F(9,36)=0.95$, $p>0.05$) although the pattern of distribution was affected ($p<0.0001$ by K-S test).

Supplemental Text

Although in previous experiments (Gal et al., 2006) we also used the same promoter and *in vivo* electroporation, we found here that the onset of the gene expression is different. We suspect the reason for this difference is that the current study uses the Cre/loxP system, which undergoes an extra step of recombination after Cre is expressed under the Tα1 promoter. The amount of Cre protein needed to exceed the threshold for recombination likely requires more time to accumulate. Hence, as shown in Figure S4A-C, Cre expression in the VZ is very weak compared to the IZ, indicating a slow accumulation of Cre protein in neuronal progenitors. Consistently, Figure S4D-H shows that the recombination was detected almost exclusively in post-mitotic neurons (EGFP overlapping with Ki67 was less than 5%). Thus, it is probable that the onset of Cre expression occurs in the neuronal progenitors but does not take full effect until neurons are post-mitotic and persists until terminal differentiation.

If signifcant genetic alteration (either deletion or overexpression) of Notch signaling occurs in neuronal progenitors, we would expect to observe altered neuronal differentiation, proliferation, radial glial fiber structure, apoptotic ratio, or gliogenesis (e.g. Gaiano et al., 2000 Neuron 26; 395-404; Yang et al., 2004 see in supplemental ref. list; Mizutani and Saito Development 2005. 132, 1295-1304; Mizutani et al., Nature 2007 449, 351-355.) However, we did not observe any of these changes in the VZ (Figures S6, S7 and S10). Thus, we suppose that the recombination in the progenitors, if any, is not substantial and has little effect in our system.

Supplemental Experimental Procedures

Constructs

Expression vectors were constructed as follows; the complementary DNA (cDNA) coding EGFP was replaced from pIRES-EGFP-N1 (BD Sciences) with the Venus cDNA (a kind gift from Dr. Miyawaki). IRES-Venus was cut out and inserted into the p253 vector including Tα1-promoter (a kind gift from Dr. Miller) to make the pTα1-IRES-Venus plasmid. Cre recombinase cDNA excised from pBS185 (Gibco BRL) was inserted into p253 or pTα1-IRES-Venus to create pTα1-Cre or pTα1-Cre-IRES-Venus. pCAG-DsRed2, pCALSL-Notch1 ICD and pCAG-GFP were described previously. We confirmed exogeneous expression of Notch1 ICD in electroporated cells (data not shown). CALSL-caRbpj was constructed by inserting FLAGRbpjVP16 (Mizutani et al., Nature 449, 351-5, 2007, a kind gift from Dr. N. Gaiano) and the polyA sequence from pCDNA3.1 into pCALSL. The activity of caRbpj was confirmed by co-electroopration with pTα1-Cre and the Rbpj-bp reporter plasmids (data not shown). PCALSL-DsRed2 was constructed by inserting DsRed2 from DsRed2-N1 construct (Clontech) and the polyA from pCDNA3.1. Mouse Dab1 expression plasmids, pCDNA3.1-mDab1 WT (wild-type) and 5YF (tagged with HA) were kind gifts from Drs. Tsai and Sanada. We confirmed the expression by using HA immunohistochemistry (data not shown). RBP-J luciferase reporter plasmid, pGL2-8xCBF-Luc, was kindly provided from Dr Hayward. PCDNA3.1-caSrc (SrcY527F) and pCDNA3.1-HA-Ub were kind gifts from Dr. Baron. pCDNA3.1 and phRL were purchased from Invitrogen and Promega, respectively. MEK kinase 4 (MEKK4) shRNA expression plasmid, pU6pro-MEKK4 shRNA #555, was described elsewhere. Myc-tagged Notch1 ICD expression plasmid, pCDNA3.1NIC1-myc, was a kind gift from Dr. Nye. pCDNA3.1-HA-hFbxw7 was kindly provided from Dr. Israël. Rbpj-bp-dVenus (originally called as TP-1) and rBG-dVenus reporter plasmids were provided by Dr. H. Okano. For reporter analysis, the plasmids were electroporated at the following concentrations: Rbpj-bp-dVenus (4mg/ml), rBG-dVenus (4mg/ml) with pCAG-DsRed2 (0.5mg/ml).

Immunohistochemistry

Brains were fixed with 4% paraformaldehyde in phosphate buffered saline overnight. 70 μm thick coronal vibratome slices or 18 μm coronal cryosections were collected. Following primary antibodies were used; polyclonal anti-Notch1 ICD (Val1744; 1:50; Cell signaling technology), anti-GFP (also recognize Venus, 1:1000; Molecular Probes), anti-DsRed (1:5000; BD Biosciences), anti-Tbr1 (1:1000; Chemicon), anti-Cutl1 (1:300 Santa Cruz Biotechnology), anti-HA (1:300, Santa Cruz Biotechnology), anti-Notch1 (1:1000; a kind gift from Dr. A Israël), anti-glial fibrillary acidic protein (Gfap) (1:500; Abcam), anti-Fbxw7 (1:100; Abcam), monoclonal Anti-NeuN (1:1,000: Chemicon) anti-RIP (1:10,000; Chemicon), anti-Ki67 (1:100; Neomarker), anti-BrdU (1:100 Beckton and Dickinson), anti-Nestin (Rat-401; 1:10; DSHB), anti-β tubulin (class III)(Tuj1; 1:200; Covance), anti-Cre recombinase (1:100; biotin conjugated clone 7.23; Covance) antibodies. Immunohistochemistry was performed using standard methods. Sections were nuclear counterstained with TO-PRO3 or DAPI (Molecular Probes) and photographed using an LSM510 confocal microscope (Zeiss).

Immunoprecipitation and Western blotting

Protein samples from E18.5 mouse brain or Cos-7 cells 2days after transfection were solubilized in ice-cold lysis buffer (Santa Cruz Biotechnology) supplemented with protease inhibitor cocktail (Roche), 10 μM MG-132 and 20 mM sodium fluoride. After 20 minutes solubilization, the cell lysates were cleared by centrifugation at 14000 rpm for 20 minutes, and the protein concentration was determined by the Bradford method. Immunoprecipitations were carried out with protein-A or -G cephalose beads bound to appropriate antibodies after precleaning of lysate by pre-incubation with appropriate beads. Polyclonal goat anti-Dab1 (E-19, N terminal domain of mouse Dab1 for antigen, Santa Cruz Biotechnology), rabbit anti-Dab1 (H-103, Santa Cruz Biotechnology), rabbit anti-Notch1 (C-20, Santa Cruz Biotechnology), rabbit anti-Notch1 (ICD) and anti-myc (9E10) antibodies were used. By using anti-Dab1 (E-19), minor isoforms of Dab1 (for example, p45) were barely precipitated (Figure 1). A nonspecific goat IgG was used for the control immunoprecipitation. The beads were washed 4 times in lysis buffer before elution. Subsequent steps of protein separation were performed using NuPAGE system with 4-12% Bis-Tris or 3-8% Tris-Acetate (for ubiquitination assays and p300 detection [Figure 1I]) gels (Invitrogen). Immunoblots were performed with subsequent antibodies; anti-Multi Ubiquitin (FK2; 1:200; MBL international), anti-β-actin (1:5000; Abcam), anti-GAPDH (1:200; chemicon), polyclonal anti-Notch1 (1:5000), anti-Notch1 (C-20) (1:200; Santa Cruz), anti-Notch1 ICD (Val1744; 1:200; Cell signaling technology), anti-Fbxw7 (1:500; Abcam) anti-Dab1 (1:5000; Abcam, ab7522), anti-GFP (1:3000; Molecular Probes). ECL plus system (Amersham Biosciences) was used to detect horseradish peroxidase-conjugated (1:5000; Bio-Rad) or biotinylated (for ubiquitination assays; 1:500; GE Healthcare) secondary antibodies. Streptavidin-biotinylated HRP was used at 1:20000 (GE Healthcare). To reprobe the membrane, Restore Western blot stripping buffer (Pierce) was used.

Quantitative RT-PCR

Primer sequences used in the study were as follows: *Notch1* (Forward) 5'-GGA TGC TGA CTG CAT GGA T, (Reverse) 5'-AAT CAT GAG GGG TGT GAA GC-3', *Hes1* (Forward) 5'-CCG AGC GTG TTG GGG AAA TAC-3', (Reverse) 5'-GTT GAT CTG GGT CAT GCA GTT GG-3', *Hes5* (Forward) 5'-GGA GAT GCT CAG TCC CAA GGA G-3', (Reverse) 5'-GCT GCT CTA TGC TGC TGT TGA TG-3'.

Supplemental References for Production of *floxed* Mice

1. Radtke, F., Wilson, A., Stark, G., Bauer, M., van Meerwijk, J., MacDonald, H.R. and Aquet, M. (1999). Deficient T cell fate specification in mice with an induced inactivation of Notch1. Immunity 10, 547-558.
2. McCright, B., Lozier, J. and Gridley, T. (2006). Generation of new Notch2 mutant alleles. Genesis *44*, 29-33.
3. Yang, X., Klein, R., Tian, X., Cheng, H.T., Kopan, R. and Shen, J. (2004). Notch activation induces apoptosis in neural progenitor cells through a p53-dependent pathway. Dev. Biol. *269,* 81-94.